



ARTICLE

Study on the Properties of Esterified Corn Starch/Poly lactide Biodegradable Blends

Yongjie Zheng^{1,2,3,*}, Mingjian Xu¹, Jingzhi Tian¹, Meihong Yu¹, Bin Tan⁴, Hong Zhao^{2,3,*} and Yin Tang^{2,3}

¹College of Chemistry and Chemical Engineering, Qiqihar University, Qiqihar, 161006, China

²Engineering Research Center of Flax Processing Technology Ministry of Education, P.R.C, Qiqihar University, Qiqihar, 161006, China

³College of Light Industry and Textile, Qiqihar University, Qiqihar, 161006, China

⁴Department of Chemical Engineering and Materials Science, Michigan State University, East Lansing, 48824, USA

*Corresponding Authors: Yongjie Zheng. Email: zyj1964@163.com; Hong Zhao. Email: hzzhao2020@163.com

Received: 09 October 2021 Accepted: 17 December 2021

ABSTRACT

Fully bio-based and biodegradable starch/poly lactic acid blends have received increasing attentions for their biodegradability and potential to offset the use of unsustainable fossil resources, specifically, their application in packaging. Herein, corn starch was first esterified with maleic anhydride and then compounded with polylactide (PLA) to prepare esterified corn starch/poly lactic acid blends with starch content up to 35 wt%. The structures, morphologies, thermal and mechanical properties of starch or blends were investigated. The results showed that corn starch was successfully grafted with maleic anhydride, which showed increased crystallinity and particle size than native starch. Esterified corn starch/poly lactic acid blends showed good surficial compatibility and good thermal stability with main decomposition temperature in the range of 300°C to 400°C. Additionally, incorporation of corn starch increased the hydrophilicity and water uptake of composites. However, the tensile and flexural strengths of blends decreased with increasing esterified starch amount.

KEYWORDS

Biodegradable polymers; corn starch; polylactide; composite

1 Introduction

Polymers have been increasingly produced since their commercial development in the 1930s, and widely used in areas including packaging, constructions, electronics and transportation. With the dramatic increase of plastics production and consumption, the world faces increasing environmental pollution of air, soil and water sources [1–4]. In recent decades, research focused on biodegradable polymers have received more and more attentions due to the promising application and the environmental consideration [5–7]. As an alternative for conventional plastics, biodegradable plastics are designed to enable biodegradation down to monomer unit, carbon dioxide, water or other biomass after the end-of-life. With increasing awareness of plastic pollution, more biodegradable plastics are required from both marketplace and government legislation. For instance, European Union is always on the front line for plastic sustainability, and ambitious to achieve 100% reusable or recyclable plastics for packaging by 2030 [8]. However, current biodegradable plastics



production and applications are quite limited due to several factors, including longer synthesizing period, higher cost or lower properties compared to conventional plastics.

Poly lactide (PLA) is one of the most used biodegradable polymers which accounts for 38% production capacity of all the global biodegradable plastics produced [9,10]. It is a promising alternative for PET and PS for short term packaging application, such as rigid containers, disposable cups, disks and films. Packaging is the largest market for PLA which accounts for more than 50%, followed by agriculture and horticulture, textiles, coatings and adhesives, and other consumer goods [11]. Most recently, PLA has been widely utilized for the emerging 3D printing technology, which accounts for 37% of all the plastics used in 3D printing production [12,13]. Due to its good biocompatibility and bioabsorbability, PLA has also been intensively explored for therapeutic and pharmaceutical applications, such as drug carrier, scaffold materials for tissue engineering and cardiovascular stent [14,15].

Starch is a native biopolymer which is cost-effective, biodegradable and widely available from agriculture [16–18]. It is composed of amylose, a linear polymer of D-glucose units attached α -1, 4-, and amylopectin, a highly branched polymer of D-glucose units attached α -1, 4-with branch points attached α -1, 6-. Starch usually presents in granular shape during biosynthesis, which have both crystalline and amorphous regions [19]. Since the glass transition temperature of starch is above its decomposition temperature, it does not soften and flow, which produces difficulty in hot processing. In addition, the existence of strong hydrogen bonds between starch molecules limits its compatibility with most polymers [20]. Usually, starch can be plasticized or destructurized by low molecules such as water, glycerol and sorbitol, which are capable for hydrogen bonding with starch molecules or destructing hydrogen bonding of starch molecules to make starch capable for hot processing or hot blending with polymers [21–24].

Blending of starch with PLA to prepare starch/PLA blends for packaging application has been explored in recently years [25–28]. Both physical and chemical methods were adopted for targeting improved interfacial compatibility and dispersion of starch in PLA matrix [29–31]. Li et al. [32] used poly (acrylic acid)-g-protein-g-poly (methyl acrylate) (PAA-g-protein-g-PMA) as an adhesive material to improve the adhesion of starch to PLA fibers. They found that blending PAA-g-protein-g-PMA with caproylated starch is an effective manner for improving the adhesion of starch to PLA fibers and ameliorating end-use issues in textile sizing and fulfilling the high-valued utilization of feather wastes. Heidemann et al. [33] used atmospheric air cold plasma as an adhesion improver between PLA and starch multiple layers and found that the best adhesion was obtained for PLA-starch film with 10 min of plasma treatment, resulting in no delamination. Zhang et al. [34], respectively, adopted pressure-induced flow (PIF) processing to assist blending of PLA and starch and found that layer-like microstructure along flow direction (FD) formed which resulted in 200% and 400% enhancement in impact and tensile strength. Xiong et al. [35] combined castor oil as plasticizer and hexamethylenediisocyanate (HDI) as grafting agent to improve the interfacial compatibility between starch and PLA, and the found that combination of castor oil and HDI dramatically improved the toughness of starch/PLA blends.

In this work, fully bio-based and biodegradable starch/poly lactic acid blends were prepared using PLA as a matrix material and maleic anhydride (MA) as a modifier. Maleic Anhydride Esterified Starch (MAES) is based on maleic anhydride starch, which is plasticized using glycerin, maleic anhydride grafted corn starch/PLA blends prepared by melt compounding. The optimized parameters for maleic anhydride grafting starch reaction were investigated, and the properties of corn starch/PLA blends with varied starch amounts were explored. With all the efforts in this work and literatures, fully bio-based and biodegradable starch/PLA blends with improved performance and reduced material cost are promoted for practical applications.

2 Experimental

2.1 Materials

Poly lactide 2003D (PLA, $M_w = 1.77 \times 10^5$ g/mol, PDI = 1.43) was purchased from NatureWorks. Corn starch and glycerol were purchased from Tianjin Tianli Chemical Reagents Co., Ltd. (China). Maleic anhydride was purchased from Tianjin Kermel Chemical Reagent Co., Ltd. (China). Acetyl tributyl citrate (ATBC) was purchased from Lanfan Chemical Reagent Co., Ltd. (China). Acetone was purchased from Quanrui Chemical Reagents Co., Ltd. (China). All the materials were used as received.

2.2 Esterification of Corn Starch

Corn starch was first dried in vacuum oven at 50°C for 3 h and then ground and sieved before use. In a typical procedure, 20 grams dried corn starch and 5 grams maleic anhydride were stirring mixed in a flame dried round bottom flask with nitrogen flow and condenser. Subsequently, the flask was heated to a specified temperature in a water bath and the esterification reaction was undergoing with designed temperature, time and maleic anhydride amount. Once the reaction was terminated and the reactants were cooled down, a acetone washing procedure was adopted by adding acetone into the flask to dissolve unreacted maleic anhydride, followed by vacuum filtered to obtain esterified starch cake. This washing procedure was repeated three times.

Aforementioned esterified starch was thoroughly dried and then mixed with glycerol with a weight ratio of 4:1 using a co-rotation twin extruder (L/D = 40). The temperature profile of the extruder from hopper to dry was set as 100°C, 105°C, 110°C, 115°C, 120°C and 115°C. The glycerol/esterified starch mixture was extruded through a 3 mm diameter die at 60 rpm, pelletized and dried for compounding with PLA.

2.3 Preparation of Esterified Starch/Poly lactide Blends

PLA was first plasticized with 1 wt% ATBC through extrusion. Specifically, PLA pellets were first wetted using ATBC, followed by extrusion through a co-rotation twin screw extruder (L/D = 40) at 45 rpm. The temperature profile of the extruder from hopper to die was set as 130°C, 160°C, 180°C, 180°C, 190°C and 180°C.

Esterified starch and plasticized PLA were compounded through extrusion with varied esterified starch amounts from 15 to 35 wt% in mass. The temperature profile of the extruder from hopper to die was set as 130°C, 160°C, 180°C, 180°C, 190°C and 180°C. The screw speed was 45 rpm. A venting port was placed closed the die to remove any volatile materials. The extruded esterified starch/PLA pellets were dried at 50°C under vacuum overnight, followed by injection molding to fabricate tensile and flexural specimens for characterizations.

2.4 Characterizations

Fourier transform infrared spectroscopy (FTIR, Spotlight400, PE Inc. (USA)) was used to measure the structure of starch at room temperature. Thin film of starch/potassium bromide powder was pressed for the FTIR measurement in the range of 500~4000 cm^{-1} . Wide angle X-ray scattering (WAXS) of starch was performed using a SmartLab X-ray diffractometer with $\text{Cu K}\alpha$ radiation.

Thermal stabilities of starch and esterified starch/PLA blends were measured using a thermo-gravimetric analyzer (PerkinElmer TGA-7) from 40°C to 600°C at a heating rate of 2 °C/min under nitrogen atmosphere. The glass transition and melting temperatures of esterified starch/PLA blends were measured using a PerkinElmer DSC-7 differential scanning calorimeter. Samples about 10 mg in weight were heated to 200°C at a rate of 10 °C/min under nitrogen atmosphere and held for 3 min to eliminate the previous thermal history. Then, the samples were cooled down to room temperature at a rate of 10 °C/min, followed by heating up to 200°C at a rate of 10 °C/min. The second heating curves were adopted for

analysis. The morphologies of starch and esterified starch/PLA blends were measured using a JAK-840 scanning electron microscope (JEOL Corporation, Japan).

The degree of esterification substitution of starch was measured using titration method. First, 5 grams esterified starch was dissolved in 50 ml deionized water and 2–3 drops of phenolphthalein test solution was added, then 0.1 M sodium hydroxide solution was gradually added until the color shifted to slight red. Subsequently, 25 ml 0.5 M sodium hydroxide solution was added with stirring for saponification. After that, 0.5 M hydrochloric acid solution was titrated until the red color disappearance. The calculation equations are as following:

$$X = \frac{98C(V_0 - V_1)}{1000 \times 2W} \quad (1)$$

$$DS(\%) = \frac{162X}{9800 - 98X} \times 100\% \quad (2)$$

where V_1 and V_0 is the consumed volume of hydrochloric acid solution by esterified starch and native starch, respectively. W is the mass of esterified starch, C is the molar concentration of hydrochloric acid solution (M), DS is the degree of esterification substitution.

Contact angle of esterified starch/PLA blends were tested using an optical contact angle tester at room temperature. The water absorption test was conducted as the following procedure. First, specimen was dried in oven until constant mass (M_0) was recorded, and then the specimen was immersed in water for 24 h at room temperature. After gently wiping off the surface water of the specimen using tissue, the mass was recorded as M_1 . The water absorption was calculated using the following equation:

$$A(\%) = \frac{M_1 - M_0}{M_0} \times 100 \quad (3)$$

where M_0 is the initial mass of specimen, M_1 is the mass of specimen after water uptake, A is water absorption in percentage.

Tensile properties of esterified starch/PLA blends were tested on an Instron model 1211 universal materials testing machine. The specimen was a dumbbell shape with the dimension of $80 \times 10 \times 4 \text{ mm}^3$, and the testing rate was 2 mm/min. The flexural properties of esterified starch/PLA blends were tested using the same machine under flexural mode. The specimen was $50 \times 10 \times 4 \text{ mm}^3$ and testing rate was 1 mm/min. All the tests were conducted at room temperature with relatively humidity of 50%, and data from five specimens were averaged as record.

3 Results and Discussion

3.1 Esterification of Corn Starch

The degree of esterification of corn starch is influenced by several parameters, including the amount of maleic anhydride, reaction temperature and time. As listed in [Table 1](#), the degree of esterification is greatly enhanced with increasing the amount of maleic anhydride. The degree of esterification increases from 0.0062% to 0.0228% when the amount of maleic anhydride increases from 0.25% to 1.5%. However, it has to be noted that maleic anhydride will evaporate if an excess of maleic anhydride is used, which reduces the efficiency of esterification. Reaction temperature also plays a crucial role on the degree of esterification. As listed in [Table 1](#), the degree of esterification linearly increases with increasing the reaction temperature from 60°C to 80°C, which increases from 0.0073% to 0.0149%. With further increasing the reaction temperature from 80°C to 100°C, the degree of esterification linearly decreases from 0.0149% to 0.0122%, due to increased evaporation rate of maleic anhydride, resulting in reduced reaction efficiency. As listed in [Table 1](#), the degree of esterification first linearly increases with increasing

the reaction time from 1 to 2 h, and then levels off with further increasing reaction time to 3 h. With these observations, it could be concluded that the optimum reaction parameters for corn starch esterification is 80°C for 2 h.

Table 1: Effects of maleic anhydride amount, reaction temperature and time on percentage of esterification

Amount of maleic anhydride (%)	2.0	1.5	1.0	0.5	0.25
Substitution (%)	0.0284	0.0228	0.0119	0.0083	0.0062
Reaction temperature (°C)	60	70	80	90	100
Substitution (%)	0.0073	0.0118	0.0149	0.0138	0.0122
Reaction time (h)	1.0	1.5	2.0	2.5	3.0
Substitution (%)	0.01276	0.01387	0.01536	0.01567	0.01586

The FTIR spectra of corn starch are presented in Fig. 1. Starch is composed of D-pyran ring structure and secondary alcoholic hydroxyl groups attached to the characteristic groups of C2 and C3, as well as the primary alcoholic hydroxyl group. As shown in Fig. 1, the asymmetric stretching vibration peak of methine protons (-CH) is around 2941 cm^{-1} ; the stretching vibration peak of hydroxyl proton (-OH) is around 3310 cm^{-1} , and the bending vibration peak of hydroxyl proton is at 625 cm^{-1} , the stretching and bending peaks of ether group (C-O-C) are around 1080 and 1155 cm^{-1} . Compared with native starch, esterified starch presents additional peaks around 1720 and 1213 cm^{-1} , due to the presence of ester bonds and incorporated ether bonds.

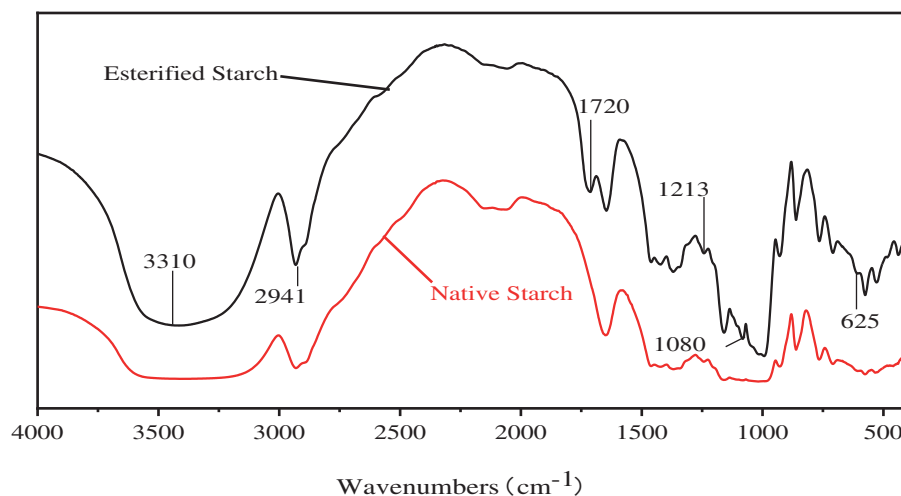


Figure 1: FTIR spectrum of native and esterified corn starch

The morphologies of native and esterified starch are presented in Fig. 2. As is shown, the native starch granules are ellipsoids with very smooth surface, while the shapes of esterified starch are irregular. It can be seen that the esterification reaction does not destroy the structure the starch, but only grafts on the surface of starch granules. This can also be confirmed from the particle size distributions of starch. The esterified starch systematically presents increased particle size than native starch. The crystal structures of starch were investigated by wide angle X-ray scattering (WAXS), as presented in Fig. 3a. The native corn starch granules exhibit A-type X-ray diffractogram with peaks at 2θ values near 15°, 17°, 18° and 22°. The pattern does not change in the esterified starch. However, the peak intensities show distinct variations for

the native and esterified starch. Esterified starch shows obviously sharper peaks. This observation can be attributed to an increase in the crystallinity induced by esterification. The thermal stability of starch is presented in Fig. 3b. It can be seen that there is around 2–5 wt% mass loss before 100°C, due to the volatilization of moisture in starch. The main loss occurs between 260°C to 400°C, with maximum decomposition rate around 300°C. There is no obvious difference in the decomposition process for native and esterified starch; the esterified starch just presents slightly more mass loss in each decomposition stage, due to the loss of esterified surfaces.

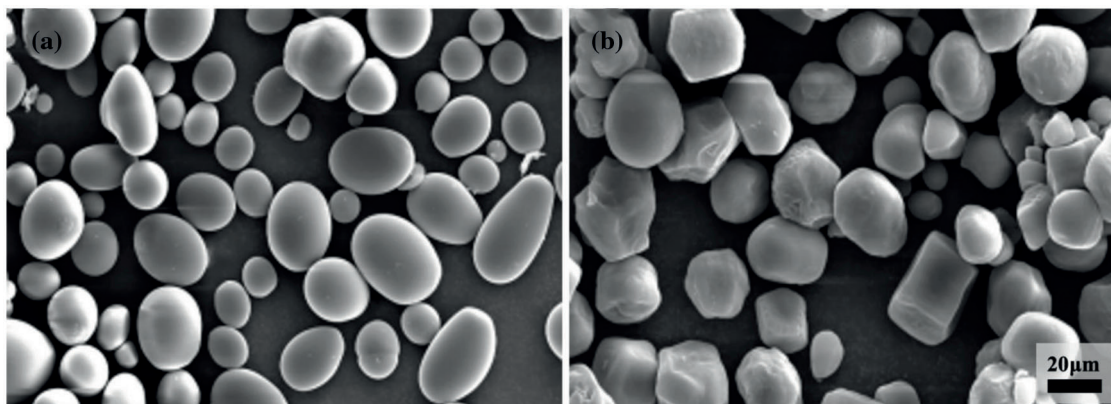


Figure 2: SEM of (a) native and (b) esterified starch

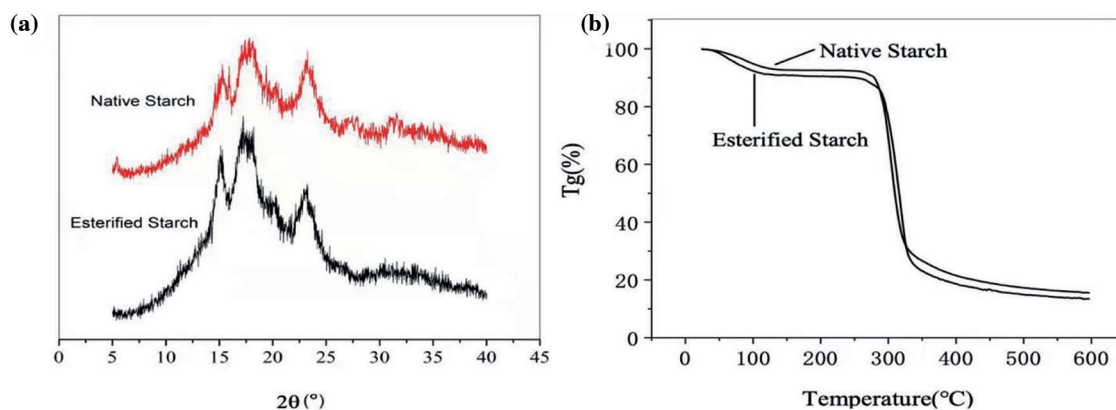


Figure 3: (a) WAXS patterns and (b) thermogravimetric curves of native and esterified starch

3.2 Properties of Esterified Starch/PLA Blends

The morphologies of esterified starch/PLA blends are presented in Fig. 4. It can be seen that the esterified starch/PLA blends illustrate good surficial compatibility with only a small portion of holes presented in the fracture surface due to separation of esterified starch particles. In addition, several esterified starch particles are also observed in the fracture surface, which also provide evidence to show good interfacial compatibility since no obvious gaps between particles and matrix are observed. Rougher surfaces and larger particle or hole sizes are also observed with increasing esterified starch amount to 30 and 35 wt%, which could be due to less efficiency in wetting esterified starch when its amount increased.

The thermogravimetric curves of pure PLA and esterified starch/PLA blends are presented in Fig. 5a. From Fig. 5a, it can be seen that pure PLA are very stable before 300°C with no mass loss, which

reveals a 10 wt% mass loss around 330°C and maximum decomposition rate around 370°C. Compared with pure PLA, esterified starch/PLA blends reveal worse thermal stability. Typically, the 10 wt% mass loss temperature decreases from around 285°C to 220°C when esterified starch is increased from 15 to 35 wt%, the maximum decomposition rate temperature also decreases from around 370°C to 320°C when esterified starch is increased from 15 to 35 wt%. Fig. 5b presents the DSC curves of pure PLA and esterified starch/PLA blends, respectively. It can be seen from Fig. 5b that pure PLA reveals a glass transition temperature at 55°C, a strong cold recrystallization peak around 110°C and melting peak at 170°C. Incorporation of esterified starch reduces the glass transition temperature of PLA down to 50°C, and shifts the melting peak to lower temperature around 150°C. In addition, broader cold recrystallization peaks are observed with increasing the amount of esterified starch, indicating reduced capability for crystallization in esterified starch/PLA blends.

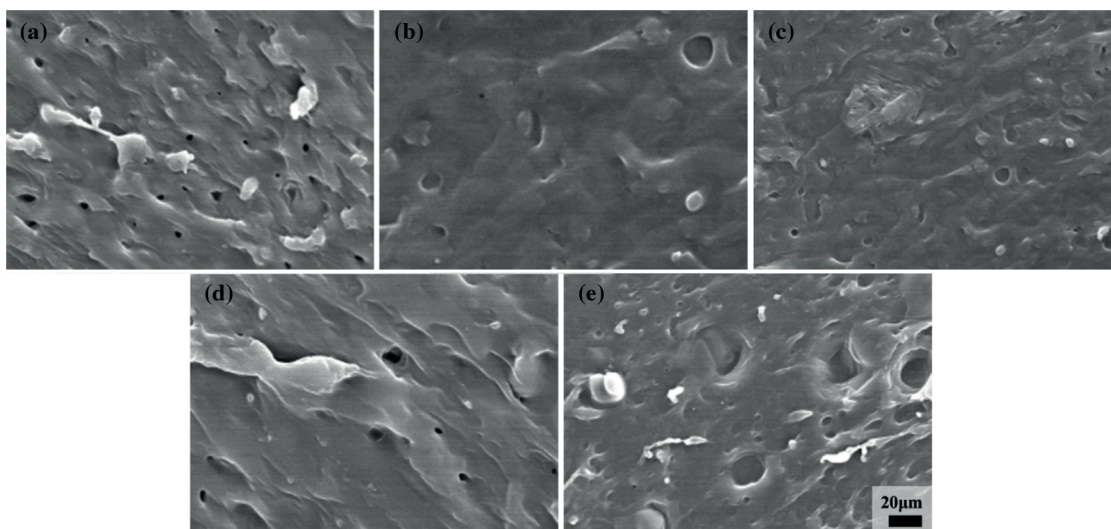


Figure 4: SEM of esterified starch/PLA blends with (a) 15, (b) 20, (c) 25, (d) 30 and (e) 35 wt% esterified starch

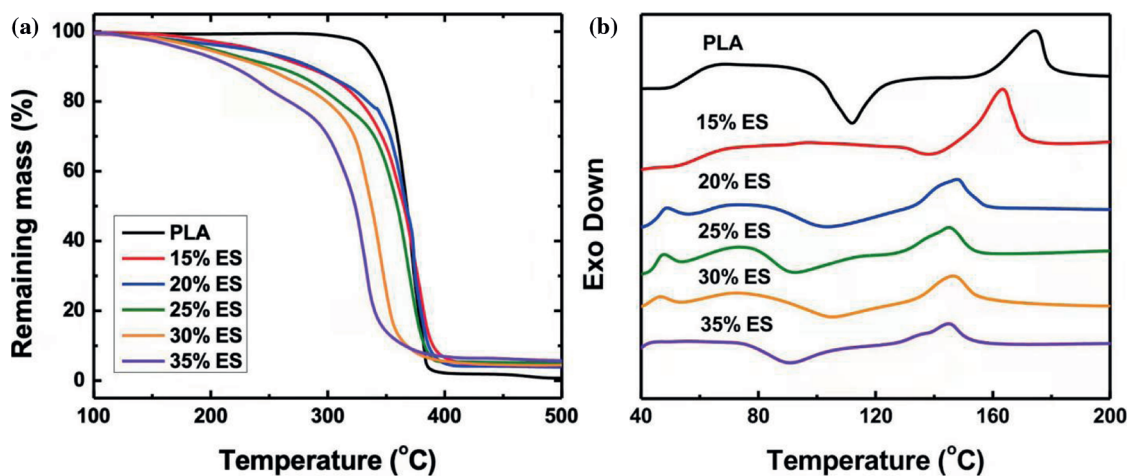


Figure 5: TGA curves of (a) pure PLA and esterified starch/PLA blends, and DSC curves of (b) pure PLA and esterified starch/PLA blends

The tensile and flexural strengths of PLA and esterified starch/PLA blends are listed in Table 2. As it can be seen that incorporation of esterified starch reduces the tensile and flexural strengths, which decrease with increasing the amount of esterified starch. The tensile and flexural strength for pure PLA is 60 and 75 MPa, respectively, which gradually decreases to 12 and 14 MPa, respectively, when 35 wt% esterified starch is incorporated. It has to be noted that incorporation of starch always reduces the mechanical properties of polymers, due to both worse mechanical properties of starch itself and compatibility issues for blends. Material merit should be considered based on cost, sustainability and required mechanical properties in applications.

Table 2: Tensile and flexural strengths of esterified starch/PLA blends

Amount of esterified starch (%)	0	15	20	25	30	35
Tensile strength (MPa)	60 ± 3.6	43 ± 3.0	37 ± 1.5	29 ± 1.4	17 ± 1.2	12 ± 1.2
Flexural strength (MPa)	75 ± 5.2	56 ± 4.5	49 ± 4.1	42 ± 2.5	17 ± 1.3	14 ± 1.0

Fig. 6 presents the contact angle of esterified starch/PLA blends with varied esterified starch amount. It can be seen that the contact angle gradually decreases with increasing esterified starch amount. The measured contact angle is 79.5°, 70.5°, 69.0°, 64.3°, 58.3° and 56.8° for pure PLA, esterified starch/PLA blends with 0, 15, 20, 25, 30 and 35 wt% esterified starch, respectively. This result shows that the existence of esterified starch shifts the surface properties of blends from being more hydrophobic to being more hydrophilic with increasing esterified starch amount. In addition, the water absorption of esterified starch/PLA blends were also tested, which is 0, 1.3%, 2.3%, 3.0%, 5.3% and 7.9% for pure PLA, esterified starch/PLA blends with 15, 20, 25, 30 and 35 wt%, respectively. All these observations show that incorporation of esterified starch increase the hydrophilicity of blends due to good hydrophilic properties of esterified starch.

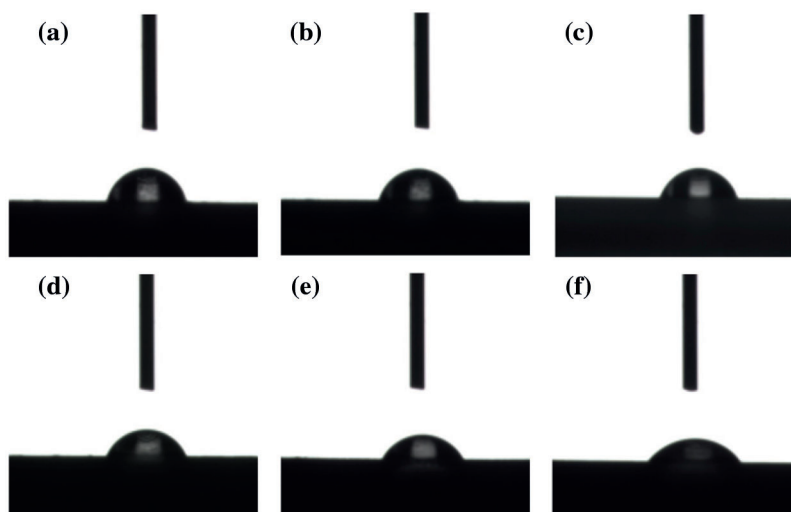


Figure 6: Contact angle of esterified starch/PLA blends with varied esterified starch amounts: (a) 0, (b) 15, (c) 20, (d) 25, (e) 30 and (f) 35 wt%

4 Conclusions

Corn starch was grafted with maleic anhydride through esterification reaction, fully bio-based and biodegradable starch/polylactic acid blends were prepared using PLA as a matrix material and maleic

anhydride (MA) as a modifier. Maleic Anhydride Esterified Starch (MAES) is based on maleic anhydride starch, which is plasticized using glycerin. The results found that the percentage of starch esterification increased with increasing maleic anhydride amount, but the most effective amount was around 1.5% and optimum reaction condition was 80°C for 2 h. Esterified starch showed larger particle size and improved crystallinity. In addition, esterified starch/PLA blends presented good surficial compatibility and stability. Increasing esterified starch amount decreased the maximum decomposition rate temperature from 370°C to 320°C when esterified starch increased from 15 to 35 wt%. The incorporation of esterified starch also decreased the tensile and flexural strengths of blends, while enhanced the hydrophilic properties and increased the water uptake.

Acknowledgement: This research was funded by the Fundamental Research Funds for Higher Education Institutions of Heilongjiang Province (135309109, 135409415) and National Natural Science Foundation of China (51803029).

Data Availability Statement: The data presented in this study are available on request from the corresponding author.

Funding Statement: The authors received no specific funding for this study.

Conflicts of Interest: The authors declare that they have no conflicts of interest to report regarding the present study.

References

1. Chae, Y., An, Y. J. (2018). Current research trends on plastic pollution and ecological impacts on the soil ecosystem: A review. *Environmental Pollution*, 240(5), 387–395. DOI 10.1016/j.envpol.2018.05.008.
2. Charitou, A., Naasan Aga-Spyridopoulou, R., Mylona, Z., Beck, R., McLellan, F. et al. (2021). Investigating the knowledge and attitude of the Greek public towards marine plastic pollution and the EU single-use plastics directive. *Marine Pollution Bulletin*, 166, 112–182. DOI 10.1016/j.marpolbul.2021.112182.
3. Bhuyan, M. S., Venkatramanan, S., Selvam, S., Szabo, S., Hossain, M. M. et al. (2021). Plastics in marine ecosystem: A review of their sources and pollution conduits. *Regional Studies in Marine Science*, 41, 101–539. DOI 10.1016/j.rsma.2020.101539.
4. Barnes, S. J. (2019). Understanding plastics pollution: The role of economic development and technological research. *Environmental Pollution*, 249(3), 812–821. DOI 10.1016/j.envpol.2019.03.108.
5. Tan, B., Bi, S., Emery, K., Sobkowicz, M. J. (2017). Bio-based poly(butylene succinate-co-hexamethylene succinate) copolyesters with tunable thermal and mechanical properties. *European Polymer Journal*, 86(11), 162–172. DOI 10.1016/j.eurpolymj.2016.11.017.
6. Zhong, Y., Godwin, P., Jin, Y., Xiao, H. (2020). Biodegradable polymers and green-based antimicrobial packaging materials: A mini-review. *Advanced Industrial and Engineering Polymer Research*, 3(11), 27–35. DOI 10.1016/j.aiepr.2019.11.002.
7. Rai, P., Mehrotra, S., Priya, S., Gnansounou, E., Sharma, S. K. (2021). Recent advances in the sustainable design and applications of biodegradable polymers. *Bioresource Technology*, 325, 124–739. DOI 10.1016/j.biortech.2021.124739.
8. Smet, D. M. (2019). *The circular economy for plastics-insights from research and innovation to inform policy and funding decisions*. Luxembourg: Publications Office of the European Union.
9. Michalski, A., Brzezinski, M., Lapienis, G., Biela, T. (2019). Star-shaped and branched polylactides: Synthesis, characterization, and properties. *Progress in Polymer Science*, 89(10), 159–212. DOI 10.1016/j.progpolymsci.2018.10.004.
10. Madhavan Nampoothiri, K., Nair, N. R., John, R. P. (2010). An overview of the recent developments in polylactide (PLA) research. *Bioresource Technology*, 101(5), 8493–8501. DOI 10.1016/j.biortech.2010.05.092.
11. European Bioplastics (2020). Bioplastics market data. <https://www.european-bioplastics.org/market>.

12. Poh, P. S. P., Chhaya, M. P., Wunner, F. M., De-Juan-Pardo, E. M., Schilling, A. F. et al. (2016). Polylactides in additive biomanufacturing. *Advanced Drug Delivery Reviews*, 107(7), 228–246. DOI 10.1016/j.addr.2016.07.006.
13. Bekas, D. G., Hou, Y., Liu, Y., Panesar, A. (2019). 3D printing to enable multifunctionality in polymer-based composites: A review. *Composites Part B: Engineering*, 179, 107–540. DOI 10.1016/j.compositesb.2019.107540.
14. Kowalczyk, P., Trzaskowska, P., Lojszczyk, I., Podgorski, R., Ciach, T. (2019). Production of 3D printed polylactide scaffolds with surface grafted hydrogel coatings. *Colloids and Surfaces B: Biointerfaces*, 179(3), 136–142. DOI 10.1016/j.colsurfb.2019.03.069.
15. Aworinde, A. K., Adeosun, S. O., Oyawale, F. A., Emagbetere, E., Ishola, F. A. et al. (2020). Comprehensive data on the mechanical properties and biodegradation profile of polylactide composites developed for hard tissue repairs. *Data in Brief*, 32, 106–107. DOI 10.1016/j.dib.2020.106107.
16. Janssen, L., Mosciacki, L. (2009). *Thermoplastic starch: A green material for various industries*, pp. 59–60. Germany: WILEY-VCH.
17. Vandevivere, L., Portier, C., Vanhoorne, V., Hausler, O., Simon, D. et al. (2019). Native starch as in situ binder for continuous twin screw wet granulation. *International Journal of Pharmaceutics*, 571, 118–760. DOI 10.1016/j.ijpharm.2019.118760.
18. Nevoralová, M., Koutný, M., Ujčič, A., Horák, P., Kredatusová, J. et al. (2019). Controlled biodegradability of functionalized thermoplastic starch based materials. *Polymer Degradation and Stability*, 170, 108–995. DOI 10.1016/j.polymdegradstab.2019.108995.
19. Chi, C., Li, X., Lu, P., Miao, S., Zhang, Y. et al. (2019). Dry heating and annealing treatment synergistically modulate starch structure and digestibility. *International Journal of Biological Macromolecules*, 137(6), 554–561. DOI 10.1016/j.ijbiomac.2019.06.137.
20. Guo, P., Li, Y., An, J., Shen, S., Dou, H. (2019). Study on structure-function of starch by asymmetrical flow field-flow fractionation coupled with multiple detectors: A review. *Carbohydrate Polymers*, 226, 115–330. DOI 10.1016/j.carbpol.2019.115330.
21. Nordin, N., Othman, S. H., Rashid, S. A., Basha, R. K. (2020). Effects of glycerol and thymol on physical, mechanical, and thermal properties of corn starch films. *Food Hydrocolloids*, 106, 105–884. DOI 10.1016/j.foodhyd.2020.105884.
22. Cheroennet, N., Pongpinyopap, S., Leejarkpai, T., Suwanmanee, U. (2017). A Trade-off between carbon and water impacts in bio-based box production chains in Thailand: A case study of PS, PLAS, PLAS/starch, and PBS. *Journal of Cleaner Production*, 167(11), 987–1001. DOI 10.1016/j.jclepro.2016.11.152.
23. Volpe, V., de Feo, G., de Marco, I., Pantani, R. (2018). Use of sunflower seed fried oil as an ecofriendly plasticizer for starch and application of this thermoplastic starch as a filler for PLA. *Industrial Crops and Products*, 122(6), 545–552. DOI 10.1016/j.indcrop.2018.06.014.
24. Ferri, J. M., Garcia-Garcia, D., Sanchez-Nacher, L., Fenollar, O., Balart, R. (2016). The effect of maleinized linseed oil (MLO) on mechanical performance of poly (lactic acid)-thermoplastic starch (PLA-TPS) blends. *Carbohydrate Polymers*, 147(3), 60–68. DOI 10.1016/j.carbpol.2016.03.082.
25. Xiong, Z., Dai, X., Zhang, R., Tang, Z., Na, H. et al. (2014). Preparation of biobased monofunctional compatibilizer from cardanol to fabricate polylactide/starch blends with superior tensile properties. *Industrial & Engineering Chemistry Research*, 53, 10653–10659. DOI 10.1021/ie500844m.
26. Zhang, J. F., Sun, X. (2004). Mechanical properties of poly (lactic acid)/starch composites compatibilized by maleic anhydride. *Biomacromolecules*, 5(4), 1446–1451. DOI 10.1021/bm0400022.
27. Wang, Y., Hu, Q., Li, T., Ma, P., Zhang, S. et al. (2018). Core-shell starch nanoparticles and their toughening of polylactide. *Industrial & Engineering Chemistry Research*, 57, 13048–13054. DOI 10.1021/ACS.IECR.8B02695.
28. Yusoff, N. H., Pal, K., Narayanan, T., de Souza, F. G. (2021). Recent trends on bioplastics synthesis and characterizations: Polylactic acid (PLA) incorporated with tapioca starch for packaging applications. *Journal of Molecular Structure*, 1232, 129954. DOI 10.1016/j.molstruc.2021.129954.
29. Ojogbo, E., Ogunsona, E. O., Mekonnen, T. H. (2020). Chemical and physical modifications of starch for renewable polymeric materials. *Materials Today Sustainability*, 7–8, 100028. DOI 10.1016/j.mtsust.2019.100028.

30. Sangeetha, V. H., Deka, H., Varghese, T. O., Nayak, S. K. (2018). State of the art and future prospectives of poly (lactic acid) based blends and composites. *Polymer Composites*, 39(1), 81101. DOI 10.1002/pc.23906.
31. Koh, J. J., Zhang, X., He, C. (2018). Fully biodegradable poly (lactic acid)/starch blends: A review of toughening strategies. *International Journal of Biological Macromolecules*, 109(12), 99–113. DOI 10.1016/j.ijbiomac.2017.12.048.
32. Li, W., Wu, Y., Xu, Z., Ni, Q., Xing, J. et al. (2020). Blending caproylated starch with poly (acrylic acid)-g-protein-g-poly (methyl acrylate) as an adhesive material to improve the adhesion of starch to PLA fibers. *International Journal of Adhesion and Adhesives*, 102, 102668. DOI 10.1016/j.ijadhadh.2020.102668.
33. Heidemann, H. M., Dotto, M. E. R., Laurindo, J. B., Carciofi, B. A. M., Costa, C. (2019). Cold plasma treatment to improve the adhesion of cassava starch films onto PCL and PLA surface. *Colloids and Surfaces A: Physicochemical and Engineering Aspects*, 580, 123739. DOI 10.1016/j.colsurfa.2019.123739.
34. Zhang, S., Feng, X., Zhu, S., Huan, Q., Han, K. et al. (2013). Novel toughening mechanism for polylactic acid (PLA)/starch blends with layer-like microstructure via pressure-induced flow (PIF) processing. *Materials Letters*, 98(12), 238–241. DOI 10.1016/j.matlet.2012.12.019.
35. Xiong, Z., Zhang, L., Ma, S., Yang, Y., Zhang, C. et al. (2013). Effect of castor oil enrichment layer produced by reaction on the properties of PLA/HDI-g-starch blends. *Carbohydrate Polymers*, 94(1), 235–243. DOI 10.1016/j.carbpol.2013.01.038.